

Questions for Flat-Minima Optimization of Modern Neural Networks

Jean Kaddour^{*1} Linqing Liu^{*1} Ricardo Silva¹ Matt J. Kusner¹

Abstract

For training neural networks, *flat-minima optimizers* that seek to find parameters in neighborhoods having uniformly low loss (flat minima) have been shown to improve upon stochastic and adaptive gradient-based methods. Two methods for finding flat minima stand out: 1. Averaging methods (i.e., Stochastic Weight Averaging, SWA), and 2. Minimax methods (i.e., Sharpness Aware Minimization, SAM). However, despite similar motivations, there has been limited investigation into their properties and no comprehensive comparison between them. In this work, we investigate the loss surfaces from a systematic benchmarking of these approaches across computer vision, natural language processing, and graph learning tasks. The results lead to a simple hypothesis: since both approaches find different flat solutions, combining them should improve generalization even further. We verify this improves over either flat-minima approach in 39 out of 42 cases. When it does not, we investigate potential reasons. We hope our results across image, graph, and text data will help researchers to improve deep learning optimizers, and practitioners to pinpoint the optimizer for the problem at hand.

1. Introduction

Stochastic gradient descent (SGD) methods are central to neural network optimization (Bottou et al., 2018). Since their initial use, there has been a wealth of research devoted to improving upon it. This includes accelerated gradient / momentum methods (Polyak, 1964; Rumelhart et al., 1988), noise reduction methods (Defazio et al., 2014; Johnson & Zhang, 2013), adaptive gradient methods (Duchi et al., 2010; Zeiler, 2012; Kingma & Ba, 2015), among others. One of the strengths of SGD-based optimizers is their ability to find so-called ‘flat’ minima: large regions that have very similar low loss values (Hochreiter & Schmidhuber, 1997). The-

^{*}Equal contribution ¹Centre for Artificial Intelligence, University College London. Correspondence to: Jean Kaddour <jean.kaddour.20@ucl.ac.uk>.

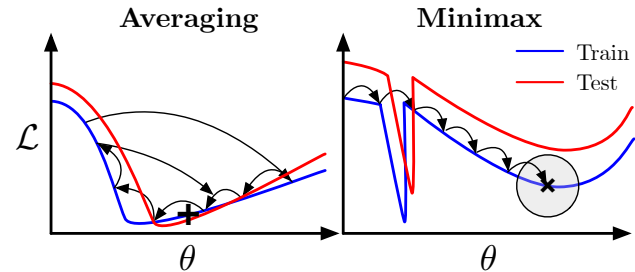


Figure 1. The motivations and mechanics behind two approaches for finding flat minima: averaging and minimax methods. The solution is denoted by + and ×, respectively. Averaging iterates produces a solution θ that is pulled towards flatter regions, while minimax methods approximate sharpness within the parameters’ neighborhood (shaded circle).

oretical and empirical studies postulate that these regions generalize well, as small shifts between the train and test distributions keep parameters in the flat (low loss) region (Dziugaite & Roy, 2017; Petzka et al., 2021; Chaudhari et al., 2017; Keskar et al., 2017; Jiang et al., 2020). This insight has caused the field of neural network optimization to shift towards developing optimizers that are explicitly designed to find such flat minima.

Flat-minima optimizers largely fall into two popular approaches: 1. Averaging methods (Polyak & Juditsky, 1992), and 2. Minimax methods (Foret et al., 2021). Averaging methods are based on the intuition that, near a minimum, flatness causes an optimizer to slow down, leaving many iterates in or around that flat region. Therefore, averaging iterates near the end of optimization will produce a solution that is pulled towards these flatter regions (see Figure 1, left)). On the other hand, minimax methods minimize the maximum loss around a neighborhood of the current iterate. This way, a region around the iterate is designed to have uniformly low loss (see Figure 1, right). These approaches have shown impressive gains over prior work. For example, flat-minima optimization can lead to similar performance gains as advanced data augmentation techniques (Chen et al., 2021a), avoiding the domain expertise required to design careful data transformations that preserve label semantics.

However, even though both approaches have the same goal, we are unaware of a systematic comparison between them.

As such, it is tricky for researchers to improve upon these approaches and for practitioners to know which approach is best for the problem at hand.

Here we fill in this missing piece by benchmarking a representative method for averaging, Stochastic Weight Averaging (SWA) (Izmailov et al., 2018), and for minimax optimization, Sharpness-Aware Minimization (SAM) (Foret et al., 2021). We select these due to their scalability to large models and excellent results across a variety of learning tasks (Nikishin et al., 2018; Athiwaratkun et al., 2019; Chen et al., 2021a; Bahri et al., 2021). This large-scale experimental study compares them across different domains (computer vision, natural language processing, graph learning), model types (multi-layer perceptrons, convolutional networks (LeCun et al., 1989), transformers (Vaswani et al., 2017)) and learning environments (classification, self-supervised learning, open-domain question answering, natural language understanding, and node/graph/link property prediction).

We analyze the loss and accuracy around and between solutions of each flat-minima approach on two prototypical settings. We find that each approach finds flat solutions in complementary ways. Better, we observe that it is possible to find flatter regions around minimax solutions, and that these regions correspond to increased accuracy. This leads us to a hypothesis: combining both approaches, a method we refer to as *weight-averaged sharpness-aware minimization* (WASAM), should further drive down generalization error. We test this hypothesis and the results confirm this: on average, taking the moving average of minimax solutions improves accuracy. In 39 out of 42 cases, WASAM performs at least as well as the worst flat-minima optimizer. When flat-minima optimizers do not help, we investigate the loss/accuracy surfaces and notice different properties compared to cases where they do (e.g., clear discrepancies between the shapes of loss and accuracy curves). To conclude, we summarize the results, and list four limitations that motivate future work directions.

2. Background and Related Work

2.1. Stochastic Gradient Descent (SGD)

The classic optimization framework of machine learning is empirical risk minimization

$$\mathcal{L}(\theta) = \frac{1}{N} \sum_{i=1}^N \ell(\mathbf{x}_i; \theta) \quad (1)$$

where $\theta \in \mathbb{R}^d$ is a vector of parameters, $\{\mathbf{x}_1, \dots, \mathbf{x}_N\}$ is a training set of inputs $\mathbf{x}_n \in \mathbb{R}^D$, and $\ell(\mathbf{x}; \theta)$ is a loss function quantifying the performance of parameters θ on \mathbf{x} .

SGD samples a minibatch $\mathcal{S} \subset \{1, \dots, N\}$ of size $|\mathcal{S}| \ll$

N from the training set and computes the gradient

$$\mathbf{g}(\theta) = \frac{1}{|\mathcal{B}|} \sum_{i \in \mathcal{B}} \nabla \ell(\theta; \mathbf{x}_i). \quad (2)$$

The parameters get updated following this gradient

$$\theta_{t+1}^{\text{SGD}} = \theta_t - \eta \mathbf{g}(\theta_t), \quad (3)$$

for a length specified by η , the learning rate. Previous research has established that this vanilla SGD training often falls into sharp minima of the loss surface (Chaudhari et al., 2017; Wang et al., 2021), in particular when the batch size $|\mathcal{B}|$ is large (Keskar et al., 2017). Most of the research improving SGD for neural networks has been devoted to reducing its sensitivity to η (Zeiler, 2012; Duchi et al., 2010; Kingma & Ba, 2015) or handling the noise introduced by minibatch sampling (Defazio et al., 2014; Johnson & Zhang, 2013). Recently, work has shifted to design optimization methods that explicitly find flat minima, often using one of two approaches: averaging or minimax optimization.

2.2. Averaging: Stochastic Weight Averaging (SWA)

The idea of averaging SGD iterates dates back to Polyak & Juditsky (1992), who proved the highest possible rates of convergence for a variety of classical optimization problems. SWA is a modern take on this idea, with the motivation being the following observation about SGD’s behavior when training neural networks: it often traverses regions of the weight space that correspond to high-performing models, but rarely reaches the central points of this optimal set. Averaging the parameter values over iterations moves the solution closer to the centroid of this space of points.

The SWA update rule is the cumulative moving average

$$\theta_{t+1}^{\text{SWA}} \leftarrow \frac{\theta_t^{\text{SWA}} \cdot k + \theta_t^{\text{SGD}}}{k + 1}, \quad (4)$$

where k is the number of distinct parameters averaged so far and t is the SGD iteration number.¹

SWA has two hyper-parameters: the update frequency ν and starting epoch E . When using a constant learning rate, Izmailov et al. (2018) suggests to update the parameters once after each epoch, i.e. $\nu \approx \frac{N}{|\mathcal{B}|}$, and starting at $E \approx 0.75T$, where T is the training budget required to train the model until convergence with conventional SGD training. SWA’s computational overhead consists of the memory requirement for an additional copy of the model weights (θ^{SWA}).

The reason for starting SWA near the end of training is that this is when SGD will most likely encounter high-performing models. He et al. (2019) postulate that SWA is effective, because most neural network loss surfaces have

¹SWA parameters are constant between averaging steps.

asymmetric sides, and SWA biases the solution towards the flatter sides (Figure 1, *left*).

Related Work (SWA) An alternative model weight averaging strategy is *exponential moving averaging*, which has been employed in deep reinforcement learning (Lillicrap et al., 2016), semi-supervised settings (Tavainen & Valpola, 2017), or image models (Wightman, 2019). Athiwaratkun et al. (2019) propose to train consistency-based methods with SWA. Maddox et al. (2019) approximate the posterior distribution over neural network weights by parameterizing a Gaussian distribution with the SWA solution as the first moment. Nikishin et al. (2018) show that SWA can improve stability in deep reinforcement learning. Cha et al. (2021) introduce a SWA variant for domain generalization tasks.

2.3. Minimax: Sharpness-Aware Minimization (SAM)

While SWA is implicitly biased towards flat minima, SAM *explicitly* approximates the flatness around parameters θ to guide the parameter update. It first computes the worst-case perturbation ϵ that maximizes the loss within a given neighborhood ρ , and then minimizes the loss w.r.t. the perturbed weights $\theta + \epsilon$.

Formally, SAM finds θ by solving the minimax problem:

$$\min_{\theta} \max_{\|\epsilon\|_2 \leq \rho} \mathcal{L}(\theta + \epsilon), \quad (5)$$

where $\rho \geq 0$ is a hyperparameter.

To find the worst-case perturbation ϵ^* efficiently in practice, Foret et al. (2021) approximates eq. (5) via a first-order Taylor expansion of $\mathcal{L}(\theta + \epsilon)$ w.r.t. ϵ around $\mathbf{0}$, obtaining

$$\epsilon^* \approx \arg \max_{\|\epsilon\|_2 \leq \rho} \epsilon^\top \nabla_{\theta} \mathcal{L}(\theta) \approx \rho \cdot \underbrace{\frac{\nabla_{\theta} \mathcal{L}(\theta)}{\|\nabla_{\theta} \mathcal{L}(\theta)\|}}_{=: \hat{\epsilon}}. \quad (6)$$

In words, $\hat{\epsilon}$ is simply the scaled gradient of the loss function w.r.t. to the current parameters θ . Given $\hat{\epsilon}$, the altered gradient used to update the current θ_t (in place of $g(\theta_t)$) is

$$\nabla_{\theta} \max_{\|\epsilon\|_2 \leq \rho} \mathcal{L}(\theta + \epsilon) \approx \nabla_{\theta} \mathcal{L}(\theta)|_{\theta + \hat{\epsilon}}.$$

Due to eq. (6), SAM’s computational overhead consists of an additional forward and backward pass per parameter update step compared to the base optimizer.

Related Work (SAM) Concurrently to Foret et al. (2021), Wu et al. (2020) propose an almost identical minimax objective, additionally including perturbations of the training data, and layer-dependent scaling of ρ . Kwon et al. (2021) propose to adaptively scale the size of the neighborhood radius ρ in relation to the model parameter’s norm to avoid

sensitivity to parameter re-scaling. Du et al. (2021) aim at reducing SAM’s computational cost by proposing two approximation strategies. Brock et al. (2021) propose to ameliorate the additional cost of eq. (6) by only employing 20% of the mini-batch to compute the gradients necessary for $\hat{\epsilon}$. Chen et al. (2021a) show that SAM is effective on Vision Transformers (ViTs) and MLP-Mixer architectures, which are more prone to land in sharp minima than ones that include convolutional layers. Bahri et al. (2021) demonstrates that SAM can improve the generalization of text-to-text transformer (T5) language models for natural language understanding and question-answering tasks.

2.4. Comparing Neural Network Minima

In this work, we aim to compare the trained models produced by the respective flat-minima optimizer, i.e. the *solutions* or *minima* found by the optimization procedure. One popular way to compare any two networks is to investigate the behavior of the loss landscape along the line between them. Previous studies successfully used such linear interpolations to gain insights and develop new methods, e.g., for training dynamics (Goodfellow & Vinyals, 2015; Frankle, 2020; Fort et al., 2020; Lucas et al., 2021; Yang et al., 2021), regularization (Li et al., 2018; Geiping et al., 2021), network pruning (Frankle et al., 2020), transfer learning (Neysshabur et al., 2020), or multitask learning (Mirzadeh et al., 2021).

If there exists no high-loss barrier between two networks along the linear interpolation, we call them (linearly) *mode-connected* or say that their solutions are located in the same *basin* (or *valley*) (Garipov et al., 2018b). Neysshabur et al. (2020) formally define the notion of two solutions being in the same basin. Informally, a basin is an area in the parameter space where the loss function has relatively low values. Due to the non-linear and compositional structure of neural networks, the linear combination of the weights of two accurate models does not necessarily define an accurate model. Hence, we generally expect high-loss barriers along the linear interpolation path.

While there are alternative distance measures that could be used to compare two networks, they typically either (a) do not offer clear interpretations, as pointed out by Frankle et al. (2020), or (b) yield trivial network connectivity results, such as *non-linear* low-loss paths, which can be found for any two network minimizers (Draxler et al., 2018; Garipov et al., 2018a; Gotmare et al., 2019; Fort & Jastrzebski, 2019).

To the best of our knowledge, prior analysis of flat-minima optimizers has only focused on verifying that they indeed find flatter solutions than non-flat² methods through sharpness measures based on the Hessian matrix of the loss func-

²We refer to optimizers not intentionally designed to find flat regions as *non-flat*, although it is not guaranteed they are sharper.

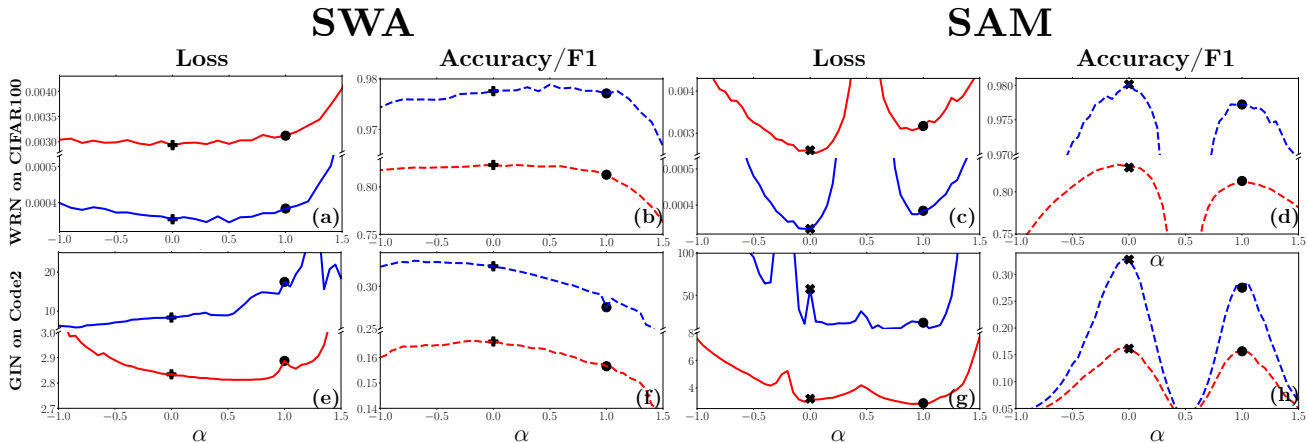


Figure 2. Training (blue) and test (red) losses (—) and accuracies (---) of linear interpolations $\theta(\alpha) = (1 - \alpha)\theta + \alpha\theta'$ (for $\alpha \in [-1, 1.5]$) between SWA (+) and SAM (x) solutions ($\alpha = 0.0$) and non-flat baseline solutions (\bullet , $\alpha = 1.0$).

tion (Chaudhari et al., 2017; Petzka et al., 2021), loss landscape visualizations generated by normally distributed direction vectors (Izmailov et al., 2018; Chen et al., 2021a) or Monte-Carlo approximations of the minimizer’s neighborhood (Foret et al., 2021; Cha et al., 2021). Instead, here we compare the surfaces of flat minima obtained by different optimizers.

3. Surfaces of Flat Minima

In this section, we investigate the loss and accuracy near the solutions of the flat-minima optimizers to understand their qualitative differences better. For two tasks where these optimizers improve over the baseline, we begin by investigating interpolations between non-flat solutions and both averaging and minimax solutions (Section 3.1). Then, we look closer at the loss/accuracy surfaces in other directions around flat solutions (Section 3.2). This leads us to our hypothesis: *SWA and SAM work in complementary ways that can be combined to improve generalization*. We end by investigating cases where flat-minima optimizers do not improve over non-flat solutions (Section 3.3).

We choose the following two disparate learning settings for analyzing flat-minima optimizers: (i) a well-known image classification task, widely used for evaluation in flat-minima optimizer papers, and (ii) a novel, challenging Python code summarization task, on which state-of-the-art models achieve only around 16% F1 score, and that has not been explored yet in the flat-minima literature. Specifically, for (i), we investigate the loss/accuracy surfaces of a WideResNet28-10 (Zagoruyko & Komodakis, 2016) model on CIFAR-100 (Krizhevsky, 2009) (baseline non-flat optimizer: SGD with momentum (SGD-M)) (Rumelhart et al., 1988). For (ii), we use the theoretically-grounded Graph Isomorphism Network (Xu et al., 2019) model on OGB-Code2

(Hu et al., 2020) (baseline optimizer: Adam (Kingma & Ba, 2015)). All optimizers start from the same initialization. We denote the minimizer produced by the non-flat methods (SGD-M and Adam) by θ^{NF} and the flat ones by θ^{SWA} and θ^{SAM} . Please see Appendix A for details on the visualizations.

3.1. What is between non-flat and flat solutions?

We start by comparing the similarity of flat and non-flat minimizers through linear interpolations. This analysis allows us to understand if they are in the same basin and how close they are to a region of sharply-increasing loss, where we expect loss/accuracy to differ widely between train and test.

Our first observation is that Figures 2a and 2e show that for both tasks, θ^{SWA} (marker: +) is in the same basin as θ^{NF} (marker: •). Additionally, when going in the direction from θ^{SWA} to θ^{NF} (i.e., $\alpha > 1$), θ^{NF} is near the periphery of a sharp increase in loss. Conversely, θ^{SWA} finds flat regions that change very slowly in loss. This finding confirms and extends those of He et al. (2019) to models beyond ResNet and PreResNet, and datasets outside of CIFAR100.

The bias of SWA to flatter loss beneficially transfers to the accuracy landscape too: Figures 2b and 2f show the accuracy/F1 score rapidly dropping off approaching and beyond θ^{NF} . Interestingly, in Figures 2e and 2f, we see that for OGB-Code2, for $\alpha < 0$, there exist solutions with even better training loss/accuracy but worse test loss/accuracy. However, θ^{SWA} is very close to the test accuracy maximizer along this interpolation (we will see in Section 5 that θ^{SWA} consistently improves over θ^{NF}).

Turning now to SAM, θ^{SAM} (marker: x) and θ^{NF} are *not* in the same basin: Figures 2c and 2g show that there is a significant loss barrier between them, respectively. This is an interesting result because we expect different basins to

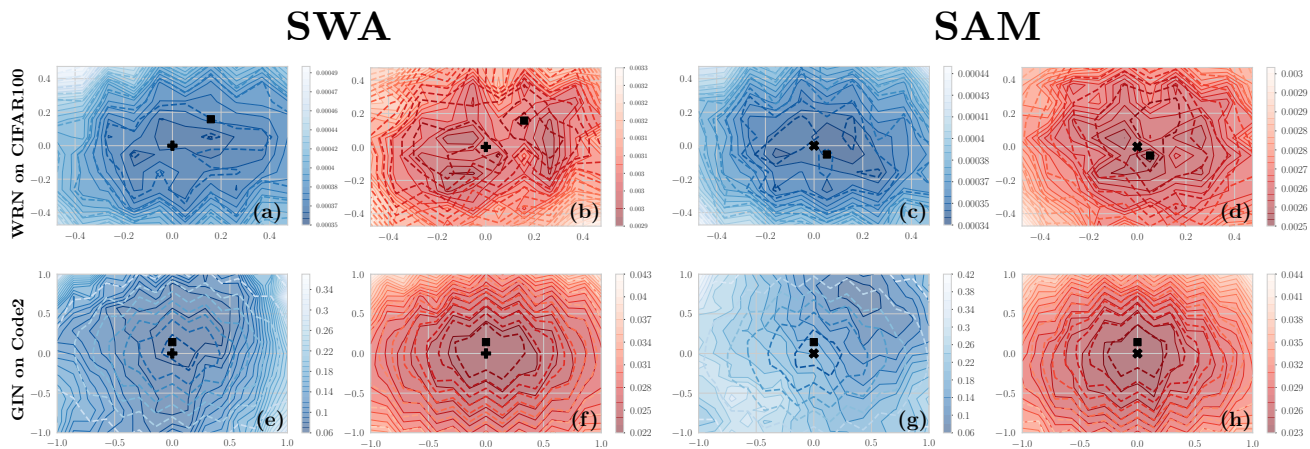


Figure 3. Are SWA and SAM solutions optimal with respect to their neighborhood? Test accuracy/F1 maximizer (■), training (blue) and test (red) losses (—) and accuracies (---) in the plane of two Gaussian random vectors around the solutions. Color-bars indicate losses.

produce qualitatively different predictions, one of the motivations behind combining models via ensembling (Huang et al., 2017; Lakshminarayanan et al., 2017). Figures 2d and 2h show that θ^{SAM} and even nearby points in parameter space achieve higher accuracies/F1 scores (i.e. generalize better) than θ^{NF} and points around it. We investigate the θ^{SAM} basin further in Section 3.2.

Lastly, another surprise is that Figure 2g shows θ^{SAM} being located in a sharp training loss minimum whose loss is much higher than θ^{NF} . Yet, its test loss is only slightly higher. On the other hand, Figure 2h shows that θ^{SAM} generalizes better w.r.t. the F1 score (the metric of interest for OGB-Code2). We give an explanation for this in the next section.

3.2. What is around flat solutions?

The linear interpolations in the previous section are instructive for differentiating flat minimization approaches. Now, we are interested in understanding if it is possible to further improve solutions by investigating them independently. Specifically, because each NN model is a point in a high-dimensional space, the loss/accuracy surface can look completely unfamiliar when starting from these same solutions but moving in different directions. Here, we investigate these different directions. Starting from the same solutions described in the previous section, we show the planes defined by two Gaussian random vectors pointing away from them. We plot the solutions of SWA (+) and SAM (x), as well as the test accuracy/F1 maximizer in the plane (■) in Figure 3.

We first observe that around the SWA solutions shown in Figures 3a and 3b (WideResNet28-10/CIFAR100) the location of the highest test accuracy is far away from the SWA solution. Further, it does not correspond to a particularly flat region of training loss or has other notable properties.

Similarly, around the SWA solutions shown in Figures 3e and 3f (GIN/OGB-Code2), the highest test F1 score point, while close to SWA, is also hard to identify: there are flatter regions (in training loss), but that correspond to worse test accuracy. It seems difficult to use the training data to improve generalization over the SWA solution (of course, this is not exhaustive evidence, as we only consider two random directions in a high-dimensional space).

For SAM, the first observation is that we have a better explanation for why the losses of θ^{SAM} are surprisingly high in Figure 2g: it finds a saddle point which is very near the maximizer of test F1, shown in Figures 3g and 3h. Additionally, around the SAM solutions, the test accuracy/F1 maximizers appear closer and seem to correspond better to flatter training loss regions. In Figures 3c and 3d, in all directions from the highest test accuracy point, the training loss increases slowly. In Figures 3g and 3h the highest test loss is right between the train loss maximizer and minimizer that make up the saddle point. This provides evidence that it may be possible to use these training signals to find flatter regions around SAM solutions, which correspond to higher test accuracy/F1.

3.3. When do flat-minima optimizers fail?

Here, we audit one case (from 3 out of 42 cases, as we will later see in Section 5), where θ^{SWA} and θ^{SAM} do not improve over θ^{NF} : training a GraphSAGE (Hamilton et al., 2017) model on OGB-Proteins: a protein-protein interaction graph where the goal is to predict the presence of protein functions (multi-label binary classification) (Hu et al., 2020). Here θ^{SWA} performs noticeably worse than flat minimizers, while θ^{SAM} performs about equally well.

Figure 4 shows two linear interpolations: between θ^{NF} (ADAM) and (1) θ^{SWA} (Figures 4a and 4b), and (2) θ^{SAM}

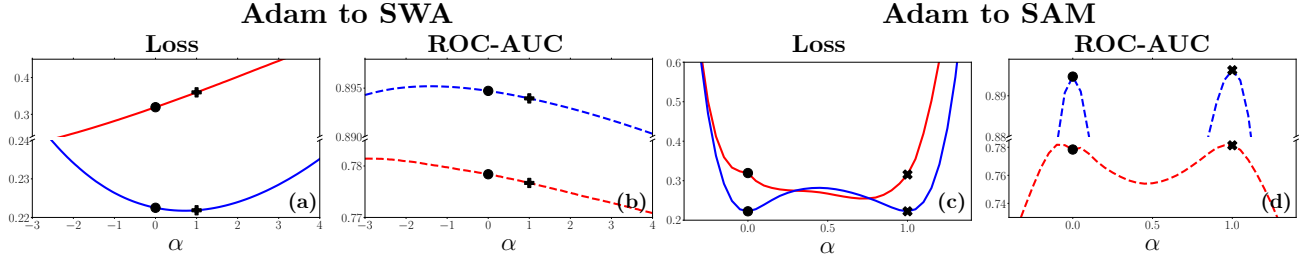


Figure 4. GraphSAGE on OGB-Proteins: Adam’s (●) solution performs about equally well as SAM (×), and better than SWA (+).

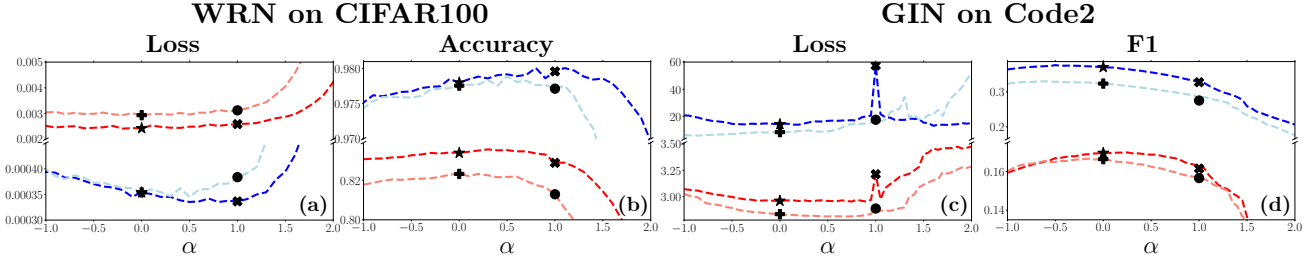


Figure 5. Training (blue) / test (red) losses (—) / accuracies (---) between non-flat baseline (●) ↔ SWA (+), SAM (×) ↔ WASAM (★).

(Figures 4c and 4d). In contrast to success cases in Figure 2, here: (a) for both SWA and SAM, the training loss minimizer is very uncorrelated with the test loss minimizer; (b) SAM and ADAM seem to be in the same test loss/accuracy basin. Investigating the causes of these we argue is a useful direction for future work.

4. Weight-Averaged SAM

In the previous section, we made three key observations: 1. SWA and SAM find different basins; 2. SWA can find flatter regions around the baseline optimizer it is averaging; 3. There exist flatter regions around SAM solutions that correspond to higher accuracy. These lead us to a hypothesis: applying the averaging technique of SWA to SAM iterates should further improve generalization. We refer to this technique as *weight-averaged sharpness-aware minimization*. Algorithm 1 describes the procedure in more detail.

Starting with the first of the two previously analyzed settings (WideResNet28-10/CIFAR100), Figures 5a, and 5b show that θ^{WASAM} (marker: ★) achieves the lowest test loss and highest test accuracy, respectively. What stands out in comparison to the previous plots is θ^{SAM} ’s (×) proximity to sharp sides, surprisingly similar to θ^{NF} (●) here and in Figures 2c and 2e.

In GIN/OGB-Code2, one unanticipated finding is that θ^{WASAM} escapes the saddle point of θ^{SAM} that we found in 3g (appearing here as a maximum), as shown in Figure 5c. This is likely because SAM traversed nearby flatter regions before arriving at the saddle point. In terms of F1

Algorithm 1 WASAM

Input: Loss function \mathcal{L} , training budget in number of iterations b , training dataset $\mathcal{D} := \cup_{i=1}^n \{\mathbf{x}_i\}$, mini-batch size $|\mathcal{B}|$, neighborhood radius ρ , averaging start epoch E , averaging frequency ν , (scheduled) learning rate η , initial weights θ_0 .

for $k \leftarrow 1, \dots, b$ **do**

 Sample a mini-batch \mathcal{B} from \mathcal{D}

 Compute worst-case perturbation $\hat{\epsilon} \leftarrow \rho \frac{\nabla \mathcal{L}(\theta)}{\|\nabla \mathcal{L}(\theta)\|_2}$

 Compute gradient $\mathbf{g} \leftarrow \nabla \mathcal{L}(\theta_t + \hat{\epsilon})$

 Update parameters $\theta_{t+1} \leftarrow \theta_t - \eta \mathbf{g}$

if $k \geq E$ and $\text{mod}(k, \nu) = 0$ **then**

$\theta_{t+1}^{\text{WASAM}} = (\theta_t^{\text{WASAM}} \cdot n + \theta_{t+1}) / (n + 1)$

end if

end for

return θ^{WASAM}

score, Figure 5d shows that while θ^{SWA} (+) and θ^{SAM} perform about equally well, the flatter region found by θ^{WASAM} improves over both.

In the same two settings we previously investigated, WASAM does not just perform as well as the best of SWA or SAM, but because of their complementary approaches to finding flatness, the combination outperforms both.

5. Benchmark Results

We compare flat minimizers SWA, SAM, and WASAM over the baseline non-flat minimizers across a range of different

tasks in the domains of computer vision, natural language processing, and graph representation learning. All results have been averaged at least three times across random seeds, and we report the corresponding standard error. We bold the best-performing approach and any approach whose average performance plus standard error overlaps it.

Hyper-parameters. For all architectures and datasets, we set hyperparameters shared by all methods (e.g., learning rate) to values cited in prior work; sometimes with minor practical modifications, e.g., adjusting the batch size to be compatible with our GPUs’ memory capacities. For flat-minima optimizers we select hyper-parameters using a grid search over a held out validation set. Specifically, for SWA we follow [Izmailov et al. \(2018\)](#) and hold the update frequency ν constant to once per epoch and tune the start time $E \in \{0.5T, 0.6T, 0.75T, 0.9T\}$ (T is the number of baseline training epochs). [Izmailov et al. \(2018\)](#) argue that in order to encourage exploration of the basin, a cyclical learning rate starting from E can help. For the sake of simplicity, we average the iterates of the baseline directly, but include even earlier starting times (i.e., $0.5T, 0.6T$). For SAM, we tune its neighborhood size $\rho \in \{0.01, 0.02, 0.05, 0.1, 0.2\}$, as in previous work ([Foret et al., 2021](#); [Bahri et al., 2021](#)).

Please see Appendix B for the values of all hyper-parameters and additional training details.

5.1. Computer Vision

Supervised Classification (SC). We evaluate the CNN architectures WideResNets ([Zagoruyko & Komodakis, 2016](#)) with 28 layers and width 10, and PyramidNet (PN) with 110 layers and widening factor 272 ([Han et al., 2017](#)) as well as Vision Transformer (ViT) ([Dosovitskiy et al., 2021](#)) and MLP-Mixer ([Tolstikhin et al., 2021](#)) on CIFAR $\{10, 100\}$ ([Krizhevsky, 2009](#)). All experiments use basic data augmentations: horizontal flip, padding by four pixels, random crop, and cutout ([Devries & Taylor, 2017](#)).

Self-Supervised Learning (SSL). We consider the following methods on CIFAR10 and ImageNette³: Momentum Contrast ([He et al., 2020](#)), a Simple framework for Contrastive Learning (SimCLR) ([Chen et al., 2020](#)), Simple Siamese representation learning (SimSiam) ([Chen & He, 2021](#)), Barlow Twins ([Zbontar et al., 2021](#)), Bootstrap your own Latent (BYOL) ([Grill et al., 2020](#)), and Swapping Assignments between multiple Views of the same image (SwAV) ([Caron et al., 2020](#)). All SSL methods use a ResNet-18 ([He et al., 2016](#)) as backbone network. To test the frozen representations, we use k -nearest-neighbor classification with a memory bank ([Wu et al., 2018](#)). We choose $k=200$ and temperature $\tau=0.1$ to reweight similarities. Compared

³<https://github.com/fastai/imagenette>

Task	Model	Baseline	SWA	SAM	WASAM
SC: CIFAR10	WRN-28-10	96.78 \pm 0.03	-0.05\pm0.04	+0.34\pm0.09	+0.25 \pm 0.05
	PN-272	96.73 \pm 0.14	+0.22 \pm 0.14	+0.42\pm0.06	+0.41\pm0.02
	ViT-B-16	98.95 \pm 0.02	-0.04\pm0.04	+0.07\pm0.01	+0.10\pm0.01
	Mixer-B-16	96.65 \pm 0.03	+0.02 \pm 0.03	+0.19\pm0.05	+0.22\pm0.06
SC: CIFAR100	WRN-28-10	80.93 \pm 0.19	+1.62 \pm 0.06	+1.82 \pm 0.14	+2.24 \pm 0.14
	PN-272	80.86 \pm 0.12	+1.88 \pm 0.04	+2.33 \pm 0.08	+2.60 \pm 0.09
	ViT-B-16	92.77 \pm 0.07	-0.12\pm0.05	+0.19\pm0.09	+0.13\pm0.07
	Mixer-B-16	83.77 \pm 0.08	+0.45 \pm 0.06	+0.52 \pm 0.15	+0.97\pm0.12
SSL: CIFAR10	MoCo	89.25\pm0.07	-0.03\pm0.10	-0.25\pm0.06	-0.17\pm0.10
	SimCLR	88.66\pm0.08	-0.05\pm0.06	+0.05\pm0.04	-0.13\pm0.06
	SimSiam	89.86\pm0.22	+0.12\pm0.26	+0.07\pm0.10	+0.11\pm0.10
	BarlowTwins	86.34\pm0.24	-0.09\pm0.19	+0.09\pm0.15	+0.14\pm0.05
	BYOL	90.32 \pm 0.14	+0.70\pm0.05	+0.14 \pm 0.03	+0.21 \pm 0.07
	SwAV	87.28 \pm 0.05	+0.09\pm0.06	+0.07\pm0.12	+0.02 \pm 0.06
SSL: ImageNette	MoCo	81.74 \pm 0.18	+0.97 \pm 0.10	+0.91 \pm 0.32	+1.40 \pm 0.10
	SimCLR	83.28 \pm 0.22	+0.95\pm0.25	+0.18 \pm 0.24	+1.07 \pm 0.13
	SimSiam	81.77 \pm 0.14	+0.20\pm0.37	+0.33\pm0.28	+0.18\pm0.26
	BarlowTwins	77.49 \pm 0.36	+0.20 \pm 0.16	+0.47\pm0.27	+0.66\pm0.57
	BYOL	84.16 \pm 0.14	+0.76\pm0.08	+0.15 \pm 0.25	+0.31 \pm 0.19
	SwAV	88.16 \pm 0.31	+1.04\pm0.27	+0.03 \pm 0.10	+1.03\pm0.09

Table 1. CV test results: Supervised Classification (SC), and Self-Supervised Learning (SSL) tasks.

to learning a linear model on top of the representations, this evaluation procedure is more robust to hyperparameter changes ([Kolesnikov et al., 2019](#)).

We observe that flat minimizers nearly always improve test accuracies for image classifications and WASAM is the best performing method in all but one case. In semi-supervised learning on CIFAR-10, the baseline non-flat optimizer is nearly always the best and the highest performing model is BYOL optimized with SWA. Whereas for ImageNette, WASAM is again the best in all but one case.

5.2. Natural Language Processing

We first consider the task of open domain question answering (ODQA) using a T5-based generative model Fusion-In-Decoder (FiD) ([Izacard & Grave, 2021](#)). We evaluate the FiD-base on the datasets of Natural Questions (NQ) ([Kwiatkowski et al., 2019](#)) and TriviaQA ([Joshi et al., 2017](#)). We also consider a range of natural language understanding tasks included in the GLUE benchmark ([Wang et al., 2018](#)), which cover acceptability, sentiment, paraphrase, similarity, and inference. We fine-tune RoBERTa-base ([Liu et al., 2019](#)) model for each task individually and report the results on the GLUE dev set.

Here the baseline non-flat optimizer and SWA are never among the most accurate. Both SAM and WASAM are the best in all but two (different) cases, only one of which is worse than the baseline.

5.3. Graph Representation Learning

We use a subset of the Open Graph Benchmark (OGB) datasets ([Hu et al., 2020](#)). The tasks are node property prediction (NPP), graph property prediction (GPP), and link

Questions for Flat-Minima Optimization of Modern Neural Networks

Task	Model	Baseline	SWA	SAM	WASAM
NQ	FiD	49.35 \pm 0.44	-0.20 \pm 0.33	+0.33 \pm 0.19	+0.48 \pm 0.21
TriviaQA	FiD	67.74 \pm 0.29	+0.40 \pm 0.24	+0.89 \pm 0.03	+0.92 \pm 0.10
COLA	RoBERTa	60.41 \pm 0.22	+0.09 \pm 0.08	+1.57 \pm 1.20	+1.41 \pm 1.14
SST	RoBERTa	94.95 \pm 0.13	-0.30 \pm 0.27	-0.23 \pm 0.40	+0.19 \pm 0.14
MRPC	RoBERTa	89.14 \pm 0.57	+0.08 \pm 0.49	+0.73 \pm 0.43	+0.81 \pm 0.38
STS _B	RoBERTa	90.40 \pm 0.02	+0.00 \pm 0.05	+0.38 \pm 0.17	+0.35 \pm 0.16
QQP	RoBERTa	91.36 \pm 0.07	+0.01 \pm 0.06	+0.08 \pm 0.07	+0.06 \pm 0.08
MNLI	RoBERTa	87.41 \pm 0.09	+0.08 \pm 0.11	+0.39 \pm 0.02	+0.35 \pm 0.03
QNLI	RoBERTa	92.96 \pm 0.06	-0.08 \pm 0.11	+0.09 \pm 0.01	+0.11 \pm 0.06
RTE	RoBERTa	80.09 \pm 0.23	-0.23 \pm 0.20	+0.70 \pm 0.65	-0.46 \pm 0.12

Table 2. NLP test results: Open-Domain Question Answering and Natural Language Understanding (GLUE) including paraphrase, sentiment analysis, and textual entailment.

Task	Model	Baseline	SWA	SAM	WASAM
NPP: Proteins	SAGE	77.79 \pm 0.18	-0.17 \pm 0.22	-0.02 \pm 0.13	-0.11 \pm 0.15
	DGCN	85.42 \pm 0.17	+0.11 \pm 0.08	-0.14 \pm 0.05	-0.08 \pm 0.07
NPP: Products	SAGE	78.92 \pm 0.08	+0.39 \pm 0.10	+0.13 \pm 0.08	+0.57 \pm 0.03
	DGCN	73.88 \pm 0.13	+0.44 \pm 0.14	+0.08 \pm 0.09	+0.53 \pm 0.05
GPP: Code2	GCN	16.04 \pm 0.09	+0.73 \pm 0.11	+0.36 \pm 0.08	+0.93 \pm 0.15
	GIN	15.73 \pm 0.11	+0.83 \pm 0.11	+0.57 \pm 0.09	+1.10 \pm 0.09
GPP: Molpcba	GIN	28.10 \pm 0.11	+0.40 \pm 0.18	-0.33 \pm 0.14	+0.33 \pm 0.16
	DGCN	25.65 \pm 0.13	+1.90 \pm 0.20	-0.13 \pm 0.18	+1.34 \pm 0.12
LPP: Biokg	CP	84.06 \pm 0.00	+0.07 \pm 0.01	0.00 \pm 0.03	+0.08 \pm 0.02
	ComplEx	84.94 \pm 0.01	+0.14 \pm 0.01	-0.02 \pm 0.01	+0.12 \pm 0.02
LPP: Citation2	GCN	79.52 \pm 0.41	-0.05 \pm 0.52	+1.32 \pm 0.06	+1.50 \pm 0.13
	SAGE	81.95 \pm 0.02	+1.15 \pm 0.02	-0.31 \pm 0.07	+0.86 \pm 0.04

Table 3. GRL test results: Node Property Prediction (NPP), Graph Property Prediction (GPP), Link Property Prediction (LPP).

property prediction (LPP). For each task, we use two of the following GNN architectures and matrix factorization methods: GCN (Kipf & Welling, 2017), DeeperGCN (DGCN) (Li et al., 2020), SAGE (Hamilton et al., 2017), GIN (Xu et al., 2019), ComplEx (Trouillon et al., 2016), and CP (Lacroix et al., 2018). We use popular training schemes, such as virtual nodes, cluster sampling (Chiang et al., 2019), or relation prediction as auxiliary training objective (Chen et al., 2021b). The reported metrics are ROC-AUC for Proteins, Accuracy for Products, F1 score for Code2, Average precision for Molpcba, and Mean Reciprocal Rank for Biokg/Citation2.

For OGB-Proteins, flatness optimization rarely helps (the first row we analyzed in Section 3.3). For all other tasks, WASAM achieves the best test scores in all but two cases. SAM is never the best performing optimizer.

5.4. Discussion

We summarize three observed trends across all domains.

1. WASAM achieves the best performance in 7 out of 8 image classification, 7 out of 12 self-supervised learning, 8 out of 10 NLP, and 8 out of 12 graph experiments.
2. There are 15 cases where only one of SWA or SAM

improves over the non-flat optimizer. In 11 of these cases, WASAM still improves over the baseline.

3. The non-flat baseline optimizer achieves the best performance only in 4 out of 12 self-supervised learning and 2 out of 12 graph experiments (6 out of 42 in total).

6. Limitations and Future Work

First, we are aware that some of the shared, fixed hyperparameter values we used in experiments may harm the effect of flat optimizers. For example, Chen et al. (2021a) note that SAM’s performance gains increase with the number of model parameters. In theory, the ideal experimental design includes tuning all hyperparameters independently for the non-flat optimizer, SWA, SAM, and WASAM. However, this design forces the number of required runs to grow exponentially in unique hyperparameters and quickly renders this benchmark infeasible. Therefore, we consider studying certain hyperparameter interactions to be important future work.

Second, there is a quickly-growing number of averaging and minimax methods that we have not investigated. For example, in the averaging category, concurrent to this work, we notice novel ways to determine the averaging period and frequency (Cha et al., 2021; Guo et al., 2022). On the minimax side, we observe new methods that primarily aim at two distinct goals: (a) to reduce the computational cost of SAM (Brock et al., 2021; Du et al., 2021; Liu et al., 2022), or (b) to improve the perturbation approximation further $\hat{\epsilon}$ (Kwon et al., 2021; Zhuang et al., 2022; Zhou & Chen, 2021). We hypothesize that improvements in each method will still produce an improved method when combined.

Third, in general, we believe fruitful directions of research include designing: (a) optimizers that explicitly find basins where training loss flatness more directly corresponds to higher hold-out accuracy, (b) post-processing methods for existing optimization runs to move into flatter regions of these basins, (c) loss functions whose contours more tightly align with accuracy contours. The results point to which tasks would most benefit from improving these things: graph learning tasks would clearly benefit from improvements in (a) (as SAM is never among the best performing method), and language tasks would benefit if (b) is improved (as SWA is never among the best performing method).

Fourth, despite our best efforts to evaluate the optimizer on a broad range of benchmark tasks, there are still plenty of unexplored domains: generative modeling, uncertainty estimation, or reinforcement learning, to name a few.

7. Conclusion

In this work, we benchmarked two representatives of flat-minima optimization methods on a diverse set of tasks (in data, learning settings, and model architectures). When they improved over the non-flat optimizers, we investigated what aspects of the training/test surfaces they were exploiting to achieve this. When they did not, we found common assumptions were broken (e.g., train and test loss minimizers being largely uncorrelated).

This investigation showed us that (a) each method found flat regions in different, orthogonal ways, and (b) there were still flat regions around SAM that could be exploited to further drive down test error. To reach these we proposed a simple idea: combine flat minimization approaches to find these flat regions. Doing so further improved generalization, an approach that performed at least as well as either flat minimizer in 39 out of 42 cases. This investigation points to directions that could further improve flat minimizers and approaches that would benefit practitioners right now, given the problem at hand.

Acknowledgements

We are very grateful to Kilian Q. Weinberger and Gao Huang for initial discussions and intuition, Pontus Stenetorp for NLP experimental design advice, and Oscar Key for feedback on the draft. JK and LL acknowledge support by the Engineering and Physical Sciences Research Council with grant number EP/S021566/1. This research was supported through Azure resources provided by The Alan Turing Institute and credits awarded by Google Cloud.

References

- Aghajanyan, A., Shrivastava, A., Gupta, A., Goyal, N., Zettlemoyer, L., and Gupta, S. Better fine-tuning by reducing representational collapse. In *International Conference on Learning Representations*, 2020.
- Athiwaratkun, B., Finzi, M., Izmailov, P., and Wilson, A. G. There are many consistent explanations of unlabeled data: Why you should average, 2019.
- Bahri, D., Mobahi, H., and Tay, Y. Sharpness-aware minimization improves language model generalization, 2021.
- Bottou, L., Curtis, F. E., and Nocedal, J. Optimization methods for large-scale machine learning. *Siam Review*, 60(2):223–311, 2018.
- Brock, A., De, S., Smith, S. L., and Simonyan, K. High-performance large-scale image recognition without normalization. In Meila, M. and Zhang, T. (eds.), *Proceedings of the 38th International Conference on Machine Learning, ICML 2021, 18-24 July 2021, Virtual Event*, volume 139 of *Proceedings of Machine Learning Research*, pp. 1059–1071. PMLR, 2021. URL <http://proceedings.mlr.press/v139/brock21a.html>.
- Caron, M., Misra, I., Mairal, J., Goyal, P., Bojanowski, P., and Joulin, A. Unsupervised learning of visual features by contrasting cluster assignments. In Larochelle, H., Ranzato, M., Hadsell, R., Balcan, M., and Lin, H. (eds.), *Advances in Neural Information Processing Systems 33: Annual Conference on Neural Information Processing Systems 2020, NeurIPS 2020, December 6-12, 2020, virtual*, 2020. URL <https://proceedings.neurips.cc/paper/2020/hash/70feb62b69f16e0238f741fab228fec2-Abstract.html>.
- Cha, J., Chun, S., Lee, K., Cho, H.-C., Park, S., Lee, Y., and Park, S. SWAD: Domain generalization by seeking flat minima. In Beygelzimer, A., Dauphin, Y., Liang, P., and Vaughan, J. W. (eds.), *Advances in Neural Information Processing Systems*, 2021. URL https://openreview.net/forum?id=zkHlu_3sJYU.
- Chaudhari, P., Choromanska, A., Soatto, S., LeCun, Y., Baldassi, C., Borgs, C., Chayes, J. T., Sagun, L., and Zecchina, R. Entropy-sgd: Biasing gradient descent into wide valleys. In *5th International Conference on Learning Representations, ICLR 2017, Toulon, France, April 24-26, 2017, Conference Track Proceedings*. OpenReview.net, 2017. URL <https://openreview.net/forum?id=B1YfAfcgl>.
- Chen, T., Kornblith, S., Norouzi, M., and Hinton, G. E. A simple framework for contrastive learning of visual representations. In *Proceedings of the 37th International Conference on Machine Learning, ICML 2020, 13-18 July 2020, Virtual Event*, volume 119 of *Proceedings of Machine Learning Research*, pp. 1597–1607. PMLR, 2020. URL <http://proceedings.mlr.press/v119/chen20j.html>.
- Chen, X. and He, K. Exploring simple siamese representation learning. In *Proceedings of the IEEE/CVF Conference on Computer Vision and Pattern Recognition*, pp. 15750–15758, 2021.
- Chen, X., Hsieh, C.-J., and Gong, B. When vision transformers outperform resnets without pre-training or strong data augmentations, 2021a.
- Chen, Y., Minervini, P., Riedel, S., and Stenetorp, P. Relation prediction as an auxiliary training objective for improving multi-relational graph representations. In *3rd Conference on Automated Knowledge Base Construction*, 2021b. URL <https://openreview.net/forum?id=Qa3uS3H7-Le>.

- Chiang, W., Liu, X., Si, S., Li, Y., Bengio, S., and Hsieh, C. Cluster-gcn: An efficient algorithm for training deep and large graph convolutional networks. In Tere-desai, A., Kumar, V., Li, Y., Rosales, R., Terzi, E., and Karypis, G. (eds.), *Proceedings of the 25th ACM SIGKDD International Conference on Knowledge Discovery & Data Mining, KDD 2019, Anchorage, AK, USA, August 4-8, 2019*, pp. 257–266. ACM, 2019. doi: 10.1145/3292500.3330925. URL <https://doi.org/10.1145/3292500.3330925>.
- Defazio, A., Bach, F. R., and Lacoste-Julien, S. SAGA: A fast incremental gradient method with support for non-strongly convex composite objectives. In Ghahramani, Z., Welling, M., Cortes, C., Lawrence, N. D., and Weinberger, K. Q. (eds.), *Advances in Neural Information Processing Systems 27: Annual Conference on Neural Information Processing Systems 2014, December 8-13 2014, Montreal, Quebec, Canada*, pp. 1646–1654, 2014. URL <https://proceedings.neurips.cc/paper/2014/hash/ede7e2b6d13a41ddf9f4bdef84fdc737-Abstract.html>.
- Deisenroth, M. P., Faisal, A. A., and Ong, C. S. *Mathematics for Machine Learning*. Cambridge University Press, 2020. doi: 10.1017/9781108679930.
- Devries, T. and Taylor, G. W. Improved regularization of convolutional neural networks with cutout. *CoRR*, abs/1708.04552, 2017. URL <http://arxiv.org/abs/1708.04552>.
- Dosovitskiy, A., Beyer, L., Kolesnikov, A., Weissenborn, D., Zhai, X., Unterthiner, T., Dehghani, M., Minderer, M., Heigold, G., Gelly, S., Uszkoreit, J., and Houlsby, N. An image is worth 16x16 words: Transformers for image recognition at scale. In *9th International Conference on Learning Representations, ICLR 2021, Virtual Event, Austria, May 3-7, 2021*. OpenReview.net, 2021. URL <https://openreview.net/forum?id=YicbFdNTTy>.
- Draxler, F., Veschgini, K., Salmhofer, M., and Hamprecht, F. A. Essentially no barriers in neural network energy landscape. In Dy, J. G. and Krause, A. (eds.), *Proceedings of the 35th International Conference on Machine Learning, ICML 2018, Stockholm, Sweden, July 10-15, 2018*, volume 80 of *Proceedings of Machine Learning Research*, pp. 1308–1317. PMLR, 2018. URL <http://proceedings.mlr.press/v80/draxler18a.html>.
- Du, J., Yan, H., Feng, J., Zhou, J. T., Zhen, L., Goh, R. S. M., and Tan, V. Y. F. Efficient sharpness-aware minimization for improved training of neural networks, 2021.
- Duchi, J. C., Hazan, E., and Singer, Y. Adaptive subgradient methods for online learning and stochastic optimization. In Kalai, A. T. and Mohri, M. (eds.), *COLT 2010 - The 23rd Conference on Learning Theory, Haifa, Israel, June 27-29, 2010*, pp. 257–269. Omnipress, 2010. URL <http://colt2010.haifa.il.ibm.com/papers/COLT2010proceedings.pdf#page=265>.
- Dziugaite, G. K. and Roy, D. M. Computing nonvacuous generalization bounds for deep (stochastic) neural networks with many more parameters than training data. In Elidan, G., Kersting, K., and Ihler, A. T. (eds.), *Proceedings of the Thirty-Third Conference on Uncertainty in Artificial Intelligence, UAI 2017, Sydney, Australia, August 11-15, 2017*. AUAI Press, 2017. URL <http://auai.org/uai2017/proceedings/papers/173.pdf>.
- Foret, P., Kleiner, A., Mobahi, H., and Neyshabur, B. Sharpness-aware minimization for efficiently improving generalization. In *9th International Conference on Learning Representations, ICLR 2021, Virtual Event, Austria, May 3-7, 2021*. OpenReview.net, 2021. URL <https://openreview.net/forum?id=6TmImposlrM>.
- Fort, S. and Jastrzebski, S. Large scale structure of neural network loss landscapes. In Wallach, H. M., Larochelle, H., Beygelzimer, A., d’Alché-Buc, F., Fox, E. B., and Garnett, R. (eds.), *Advances in Neural Information Processing Systems 32: Annual Conference on Neural Information Processing Systems 2019, NeurIPS 2019, December 8-14, 2019, Vancouver, BC, Canada*, pp. 6706–6714, 2019. URL <https://proceedings.neurips.cc/paper/2019/hash/48042b1dae4950fef2bd2aafa0b971a1-Abstract.html>.
- Fort, S., Dziugaite, G. K., Paul, M., Kharaghani, S., Roy, D. M., and Ganguli, S. Deep learning versus kernel learning: an empirical study of loss landscape geometry and the time evolution of the neural tangent kernel. In Larochelle, H., Ranzato, M., Hadsell, R., Balcan, M., and Lin, H. (eds.), *Advances in Neural Information Processing Systems 33: Annual Conference on Neural Information Processing Systems 2020, NeurIPS 2020, December 6-12, 2020, virtual*, 2020. URL <https://proceedings.neurips.cc/paper/2020/hash/405075699f065e43581f27d67bb68478-Abstract.html>.
- Frankle, J. Revisiting “qualitatively characterizing neural network optimization problems”. *CoRR*, abs/2012.06898, 2020. URL <https://arxiv.org/abs/2012.06898>.

- Frankle, J., Dziugaite, G. K., Roy, D. M., and Carbin, M. Linear mode connectivity and the lottery ticket hypothesis. In *Proceedings of the 37th International Conference on Machine Learning, ICML 2020, 13-18 July 2020, Virtual Event*, volume 119 of *Proceedings of Machine Learning Research*, pp. 3259–3269. PMLR, 2020. URL <http://proceedings.mlr.press/v119/frankle20a.html>.
- Garipov, T., Izmailov, P., Podoprikin, D., Vetrov, D. P., and Wilson, A. G. Loss surfaces, mode connectivity, and fast ensembling of dnns. In *Advances in Neural Information Processing Systems*, 2018a.
- Garipov, T., Izmailov, P., Podoprikin, D., Vetrov, D. P., and Wilson, A. G. Loss surfaces, mode connectivity, and fast ensembling of dnns. In Bengio, S., Wallach, H. M., Larochelle, H., Grauman, K., Cesa-Bianchi, N., and Garnett, R. (eds.), *Advances in Neural Information Processing Systems 31: Annual Conference on Neural Information Processing Systems 2018, NeurIPS 2018, December 3-8, 2018, Montréal, Canada*, pp. 8803–8812, 2018b. URL <https://proceedings.neurips.cc/paper/2018/hash/be3087e74e9100d4bc4c6268cdbc8456-Abstract.html>.
- Geiping, J., Goldblum, M., Pope, P. E., Moeller, M., and Goldstein, T. Stochastic training is not necessary for generalization. *CoRR*, abs/2109.14119, 2021. URL <https://arxiv.org/abs/2109.14119>.
- Goodfellow, I. J. and Vinyals, O. Qualitatively characterizing neural network optimization problems. In Bengio, Y. and LeCun, Y. (eds.), *3rd International Conference on Learning Representations, ICLR 2015, San Diego, CA, USA, May 7-9, 2015, Conference Track Proceedings*, 2015. URL <http://arxiv.org/abs/1412.6544>.
- Gotmare, A., Keskar, N. S., Xiong, C., and Socher, R. A closer look at deep learning heuristics: Learning rate restarts, warmup and distillation. In *7th International Conference on Learning Representations, ICLR 2019, New Orleans, LA, USA, May 6-9, 2019*. OpenReview.net, 2019. URL <https://openreview.net/forum?id=r14EOsCqKX>.
- Grill, J., Strub, F., Alché, F., Tallec, C., Richemond, P. H., Buchatskaya, E., Doersch, C., Pires, B. Á., Guo, Z., Azar, M. G., Piot, B., Kavukcuoglu, K., Munos, R., and Valko, M. Bootstrap your own latent - A new approach to self-supervised learning. In Larochelle, H., Ranzato, M., Hadsell, R., Balcan, M., and Lin, H. (eds.), *Advances in Neural Information Processing Systems 33: Annual Conference on Neural Information Processing Systems 2020, NeurIPS 2020, December 6-12, 2020, virtual*, 2020. URL <https://proceedings.neurips.cc/paper/2020/hash/f3ada80d5c4ee70142b17b8192b2958e-Abstract.html>.
- Guo, H., Jin, J., and Liu, B. Stochastic weight averaging revisited. *CoRR*, abs/2201.00519, 2022. URL <https://arxiv.org/abs/2201.00519>.
- Hamilton, W. L., Ying, R., and Leskovec, J. Inductive representation learning on large graphs. In *Proceedings of the 31st International Conference on Neural Information Processing Systems*, pp. 1025–1035, 2017.
- Han, D., Kim, J., and Kim, J. Deep pyramidal residual networks. In *2017 IEEE Conference on Computer Vision and Pattern Recognition, CVPR 2017, Honolulu, HI, USA, July 21-26, 2017*, pp. 6307–6315. IEEE Computer Society, 2017. doi: 10.1109/CVPR.2017.668. URL <https://doi.org/10.1109/CVPR.2017.668>.
- He, H., Huang, G., and Yuan, Y. Asymmetric valleys: Beyond sharp and flat local minima. In Wallach, H. M., Larochelle, H., Beygelzimer, A., d’Alché-Buc, F., Fox, E. B., and Garnett, R. (eds.), *Advances in Neural Information Processing Systems 32: Annual Conference on Neural Information Processing Systems 2019, NeurIPS 2019, December 8-14, 2019, Vancouver, BC, Canada*, pp. 2549–2560, 2019. URL <https://proceedings.neurips.cc/paper/2019/hash/01d8bae291b1e4724443375634ccfa0e-Abstract.html>.
- He, K., Zhang, X., Ren, S., and Sun, J. Deep residual learning for image recognition. In *2016 IEEE Conference on Computer Vision and Pattern Recognition, CVPR 2016, Las Vegas, NV, USA, June 27-30, 2016*, pp. 770–778. IEEE Computer Society, 2016. doi: 10.1109/CVPR.2016.90. URL <https://doi.org/10.1109/CVPR.2016.90>.
- He, K., Fan, H., Wu, Y., Xie, S., and Girshick, R. B. Momentum contrast for unsupervised visual representation learning. In *2020 IEEE/CVF Conference on Computer Vision and Pattern Recognition, CVPR 2020, Seattle, WA, USA, June 13-19, 2020*, pp. 9726–9735. Computer Vision Foundation / IEEE, 2020. doi: 10.1109/CVPR42600.2020.00975. URL <https://doi.org/10.1109/CVPR42600.2020.00975>.
- Hochreiter, S. and Schmidhuber, J. Flat minima. *Neural computation*, 9(1):1–42, 1997.
- Hu, W., Fey, M., Zitnik, M., Dong, Y., Ren, H., Liu, B., Catasta, M., and Leskovec, J. Open graph benchmark: Datasets for machine learning on graphs. In Larochelle,

- H., Ranzato, M., Hadsell, R., Balcan, M., and Lin, H. (eds.), *Advances in Neural Information Processing Systems 33: Annual Conference on Neural Information Processing Systems 2020, NeurIPS 2020, December 6-12, 2020, virtual*, 2020. URL <https://proceedings.neurips.cc/paper/2020/hash/fb60d411a5c5b72b2e7d3527cfc84fd0-Abstract./openreview.net/forum?id=HloyRlYgg.html>.
- Huang, G., Li, Y., Pleiss, G., Liu, Z., Hopcroft, J. E., and Weinberger, K. Q. Snapshot ensembles: Train 1, get M for free. In *5th International Conference on Learning Representations, ICLR 2017, Toulon, France, April 24-26, 2017, Conference Track Proceedings*. OpenReview.net, 2017. URL <https://openreview.net/forum?id=BJYwwY911>.
- Izacard, G. and Grave, É. Leveraging passage retrieval with generative models for open domain question answering. In *Proceedings of the 16th Conference of the European Chapter of the Association for Computational Linguistics: Main Volume*, pp. 874–880, 2021.
- Izmailov, P., Podoprikin, D., Garipov, T., Vetrov, D. P., and Wilson, A. G. Averaging weights leads to wider optima and better generalization. In Globerson, A. and Silva, R. (eds.), *Proceedings of the Thirty-Fourth Conference on Uncertainty in Artificial Intelligence, UAI 2018, Monterey, California, USA, August 6-10, 2018*, pp. 876–885. AUAI Press, 2018. URL <http://auai.org/uai2018/proceedings/papers/313.pdf>.
- Jiang, Y., Neyshabur, B., Mobahi, H., Krishnan, D., and Bengio, S. Fantastic generalization measures and where to find them. In *8th International Conference on Learning Representations, ICLR 2020, Addis Ababa, Ethiopia, April 26-30, 2020*. OpenReview.net, 2020. URL <https://openreview.net/forum?id=SJgIPJBFvH>.
- Johnson, R. and Zhang, T. Accelerating stochastic gradient descent using predictive variance reduction. In Burges, C. J. C., Bottou, L., Ghahramani, Z., and Weinberger, K. Q. (eds.), *Advances in Neural Information Processing Systems 26: 27th Annual Conference on Neural Information Processing Systems 2013. Proceedings of a meeting held December 5-8, 2013, Lake Tahoe, Nevada, United States*, pp. 315–323, 2013. URL <https://proceedings.neurips.cc/paper/2013/hash/ac1dd209cbcc5e5d1c6e28598e8cbbe8-Abstract.html>.
- Joshi, M., Choi, E., Weld, D. S., and Zettlemoyer, L. Triviaqa: A large scale distantly supervised challenge dataset for reading comprehension. In *Proceedings of the 55th Annual Meeting of the Association for Computational Linguistics (Volume 1: Long Papers)*, pp. 1601–1611, 2017.
- Keskar, N. S., Mudigere, D., Nocedal, J., Smelyanskiy, M., and Tang, P. T. P. On large-batch training for deep learning: Generalization gap and sharp minima. In *5th International Conference on Learning Representations, ICLR 2017, Toulon, France, April 24-26, 2017, Conference Track Proceedings*. OpenReview.net, 2017. URL <https://openreview.net/forum?id=HloyRlYgg>.
- Kingma, D. P. and Ba, J. Adam: A method for stochastic optimization. In Bengio, Y. and LeCun, Y. (eds.), *3rd International Conference on Learning Representations, ICLR 2015, San Diego, CA, USA, May 7-9, 2015, Conference Track Proceedings*, 2015. URL <http://arxiv.org/abs/1412.6980>.
- Kipf, T. N. and Welling, M. Semi-supervised classification with graph convolutional networks. In *5th International Conference on Learning Representations, ICLR 2017, Toulon, France, April 24-26, 2017, Conference Track Proceedings*. OpenReview.net, 2017. URL <https://openreview.net/forum?id=SJU4ayYgl>.
- Kolesnikov, A., Zhai, X., and Beyer, L. Revisiting self-supervised visual representation learning. In *Proceedings of the IEEE/CVF conference on computer vision and pattern recognition*, pp. 1920–1929, 2019.
- Krizhevsky, A. Learning multiple layers of features from tiny images. Technical report, University of Toronto, 2009.
- Kwiatkowski, T., Palomaki, J., Redfield, O., Collins, M., Parikh, A., Alberti, C., Epstein, D., Polosukhin, I., Devlin, J., Lee, K., et al. Natural questions: A benchmark for question answering research. *Transactions of the Association for Computational Linguistics*, 7:452–466, 2019.
- Kwon, J., Kim, J., Park, H., and Choi, I. K. Asam: Adaptive sharpness-aware minimization for scale-invariant learning of deep neural networks. In Meila, M. and Zhang, T. (eds.), *Proceedings of the 38th International Conference on Machine Learning*, volume 139 of *Proceedings of Machine Learning Research*, pp. 5905–5914. PMLR, 18–24 Jul 2021. URL <https://proceedings.mlr.press/v139/kwon21b.html>.
- Lacroix, T., Usunier, N., and Obozinski, G. Canonical tensor decomposition for knowledge base completion. In Dy, J. G. and Krause, A. (eds.), *Proceedings of the 35th International Conference on Machine Learning, ICML 2018, Stockholmsmässan, Stockholm, Sweden, July 10-15, 2018*, volume 80 of *Proceedings of Machine Learning Research*, pp. 2869–2878. PMLR, 2018. URL <http://proceedings.mlr.press/v80/lacroix18a.html>.

- Lakshminarayanan, B., Pritzel, A., and Blundell, C. Simple and scalable predictive uncertainty estimation using deep ensembles. In Guyon, I., von Luxburg, U., Bengio, S., Wallach, H. M., Fergus, R., Vishwanathan, S. V. N., and Garnett, R. (eds.), *Advances in Neural Information Processing Systems 30: Annual Conference on Neural Information Processing Systems 2017, December 4-9, 2017, Long Beach, CA, USA*, pp. 6402–6413, 2017. URL <https://proceedings.neurips.cc/paper/2017/hash/9ef2ed4b7fd2c810847ffa5fa85bce38-Abstract.html>.
- LeCun, Y., Boser, B., Denker, J., Henderson, D., Howard, R., Hubbard, W., and Jackel, L. Handwritten digit recognition with a back-propagation network. *Advances in neural information processing systems*, 2, 1989.
- Li, G., Xiong, C., Thabet, A., and Ghanem, B. Deepergcn: All you need to train deeper gcns, 2020.
- Li, H., Xu, Z., Taylor, G., Studer, C., and Goldstein, T. Visualizing the loss landscape of neural nets. In Bengio, S., Wallach, H. M., Larochelle, H., Grauman, K., Cesa-Bianchi, N., and Garnett, R. (eds.), *Advances in Neural Information Processing Systems 31: Annual Conference on Neural Information Processing Systems 2018, NeurIPS 2018, December 3-8, 2018, Montréal, Canada*, pp. 6391–6401, 2018. URL <https://proceedings.neurips.cc/paper/2018/hash/a41b3bb3e6b050b6c9067c67f663b915-Abstract.html>.
- Lillicrap, T. P., Hunt, J. J., Pritzel, A., Heess, N., Erez, T., Tassa, Y., Silver, D., and Wierstra, D. Continuous control with deep reinforcement learning. In Bengio, Y. and LeCun, Y. (eds.), *4th International Conference on Learning Representations, ICLR 2016, San Juan, Puerto Rico, May 2-4, 2016, Conference Track Proceedings*, 2016. URL <http://arxiv.org/abs/1509.02971>.
- Liu, Y., Ott, M., Goyal, N., Du, J., Joshi, M., Chen, D., Levy, O., Lewis, M., Zettlemoyer, L., and Stoyanov, V. Roberta: A robustly optimized bert pretraining approach. *arXiv preprint arXiv:1907.11692*, 2019.
- Liu, Y., Mai, S., Chen, X., Hsieh, C.-J., and You, Y. Sharpness-aware minimization in large-batch training: Training vision transformer in minutes, 2022. URL https://openreview.net/forum?id=7VYh_3ZD84.
- Lucas, J., Bae, J., Zhang, M. R., Fort, S., Zemel, R. S., and Grosse, R. B. Analyzing monotonic linear interpolation in neural network loss landscapes. *CoRR*, abs/2104.11044, 2021. URL <https://arxiv.org/abs/2104.11044>.
- Maddox, W., Garipov, T., Izmailov, P., Vetrov, D., and Wilson, A. G. A simple baseline for bayesian uncertainty in deep learning, 2019.
- Mirzadeh, S., Farajtabar, M., Görür, D., Pascanu, R., and Ghasemzadeh, H. Linear mode connectivity in multi-task and continual learning. In *9th International Conference on Learning Representations, ICLR 2021, Virtual Event, Austria, May 3-7, 2021*. OpenReview.net, 2021. URL https://openreview.net/forum?id=Fmg_fQYUejf.
- Neyshabur, B., Sedghi, H., and Zhang, C. What is being transferred in transfer learning? In Larochelle, H., Ranzato, M., Hadsell, R., Balcan, M., and Lin, H. (eds.), *Advances in Neural Information Processing Systems 33: Annual Conference on Neural Information Processing Systems 2020, NeurIPS 2020, December 6-12, 2020, virtual*, 2020. URL <https://proceedings.neurips.cc/paper/2020/hash/0607f4c705595b911a4f3e7a127b44e0-Abstract.html>.
- Nikishin, E., Izmailov, P., Athiwaratkun, B., Podoprikin, D., Garipov, T., Shvechikov, P., Vetrov, D., and Wilson, A. G. Improving stability in deep reinforcement learning with weight averaging. In *Uncertainty in artificial intelligence workshop on uncertainty in Deep learning*, 2018.
- Petzka, H., Kamp, M., Adilova, L., Sminchisescu, C., and Boley, M. Relative flatness and generalization. In *Thirty-Fifth Conference on Neural Information Processing Systems*, 2021. URL https://openreview.net/forum?id=sygvo7ctb_.
- Polyak, B. T. Some methods of speeding up the convergence of iteration methods. *Ussr computational mathematics and mathematical physics*, 4(5):1–17, 1964.
- Polyak, B. T. and Juditsky, A. B. Acceleration of stochastic approximation by averaging. *SIAM journal on control and optimization*, 30(4):838–855, 1992.
- Rumelhart, D. E., Hinton, G. E., and Williams, R. J. *Learning Representations by Back-Propagating Errors*, pp. 696–699. MIT Press, Cambridge, MA, USA, 1988. ISBN 0262010976.
- Susmelj, I., Heller, M., Wirth, P., Prescott, J., and et al., M. E. Lightly. *GitHub. Note: https://github.com/lightly-ai/lightly*, 2020.
- Tarvainen, A. and Valpola, H. Mean teachers are better role models: Weight-averaged consistency targets improve semi-supervised deep learning results. In Guyon, I., von Luxburg, U., Bengio, S., Wallach, H. M., Fergus, R.,

- Vishwanathan, S. V. N., and Garnett, R. (eds.), *Advances in Neural Information Processing Systems 30: Annual Conference on Neural Information Processing Systems 2017, December 4-9, 2017, Long Beach, CA, USA*, pp. 1195–1204, 2017. URL <https://proceedings.neurips.cc/paper/2017/hash/68053af2923e00204c3ca7c6a3150cf7-Abstract.html>.
- Tolstikhin, I. O., Houlsby, N., Kolesnikov, A., Beyer, L., Zhai, X., Unterthiner, T., Yung, J., Steiner, A., Keysers, D., Uszkoreit, J., Lucic, M., and Dosovitskiy, A. Mlp-mixer: An all-mlp architecture for vision. *CoRR*, abs/2105.01601, 2021. URL <https://arxiv.org/abs/2105.01601>.
- Trouillon, T., Welbl, J., Riedel, S., Gaussier, É., and Bouchard, G. Complex embeddings for simple link prediction. In Balcan, M. and Weinberger, K. Q. (eds.), *Proceedings of the 33rd International Conference on Machine Learning, ICML 2016, New York City, NY, USA, June 19-24, 2016*, volume 48 of *JMLR Workshop and Conference Proceedings*, pp. 2071–2080. JMLR.org, 2016. URL <http://proceedings.mlr.press/v48/trouillon16.html>.
- Vaswani, A., Shazeer, N., Parmar, N., Uszkoreit, J., Jones, L., Gomez, A. N., Kaiser, Ł., and Polosukhin, I. Attention is all you need. In *Advances in neural information processing systems*, pp. 5998–6008, 2017.
- Wang, A., Singh, A., Michael, J., Hill, F., Levy, O., and Bowman, S. Glue: A multi-task benchmark and analysis platform for natural language understanding. In *Proceedings of the 2018 EMNLP Workshop BlackboxNLP: Analyzing and Interpreting Neural Networks for NLP*, pp. 353–355, 2018.
- Wang, X., Oh, S., and Rhee, C. Eliminating sharp minima from SGD with truncated heavy-tailed noise. *CoRR*, abs/2102.04297, 2021. URL <https://arxiv.org/abs/2102.04297>.
- Wightman, R. Pytorch image models. <https://github.com/rwightman/pytorch-image-models>, 2019.
- Wolf, T., Chaumond, J., Debut, L., Sanh, V., Delangue, C., Moi, A., Cistac, P., Funtowicz, M., Davison, J., Shleifer, S., et al. Transformers: State-of-the-art natural language processing. In *Proceedings of the 2020 Conference on Empirical Methods in Natural Language Processing: System Demonstrations*, pp. 38–45, 2020.
- Wu, D., Xia, S., and Wang, Y. Adversarial weight perturbation helps robust generalization. In Larochelle, H., Ranzato, M., Hadsell, R., Balcan, M., and Lin, H. (eds.), *Advances in Neural Information Processing Systems 33: Annual Conference on Neural Information Processing Systems 2020, NeurIPS 2020, December 6-12, 2020, virtual*, 2020. URL <https://proceedings.neurips.cc/paper/2020/hash/1ef91c212e30e14bf125e9374262401f-Abstract.html>.
- Wu, Z., Xiong, Y., Yu, S. X., and Lin, D. Unsupervised feature learning via non-parametric instance discrimination. In *2018 IEEE Conference on Computer Vision and Pattern Recognition, CVPR 2018, Salt Lake City, UT, USA, June 18-22, 2018*, pp. 3733–3742. Computer Vision Foundation / IEEE Computer Society, 2018. doi: 10.1109/CVPR.2018.00393. URL http://openaccess.thecvf.com/content_cvpr_2018/html/Wu_Unsupervised_Feature_Learning_CVPR_2018_paper.html.
- Xu, K., Hu, W., Leskovec, J., and Jegelka, S. How powerful are graph neural networks? In *7th International Conference on Learning Representations, ICLR 2019, New Orleans, LA, USA, May 6-9, 2019*. OpenReview.net, 2019. URL <https://openreview.net/forum?id=ryGs6iA5Km>.
- Yang, Y., Hodgkinson, L., Theisen, R., Zou, J., Gonzalez, J. E., Ramchandran, K., and Mahoney, M. W. Taxonomizing local versus global structure in neural network loss landscapes. In Beygelzimer, A., Dauphin, Y., Liang, P., and Vaughan, J. W. (eds.), *Advances in Neural Information Processing Systems*, 2021. URL <https://openreview.net/forum?id=P6bUrLREcne>.
- Zagoruyko, S. and Komodakis, N. Wide residual networks. In Wilson, R. C., Hancock, E. R., and Smith, W. A. P. (eds.), *Proceedings of the British Machine Vision Conference 2016, BMVC 2016, York, UK, September 19-22, 2016*. BMVA Press, 2016. URL <http://www.bmva.org/bmvc/2016/papers/paper087/index.html>.
- Zbontar, J., Jing, L., Misra, I., LeCun, Y., and Deny, S. Barlow twins: Self-supervised learning via redundancy reduction. In Meila, M. and Zhang, T. (eds.), *Proceedings of the 38th International Conference on Machine Learning, ICML 2021, 18-24 July 2021, Virtual Event*, volume 139 of *Proceedings of Machine Learning Research*, pp. 12310–12320. PMLR, 2021. URL <http://proceedings.mlr.press/v139/zbontar21a.html>.
- Zeiler, M. D. ADADELTA: an adaptive learning rate method. *CoRR*, abs/1212.5701, 2012. URL <http://arxiv.org/abs/1212.5701>.

Zhou, W. and Chen, M. δ -sam: Sharpness-aware minimization with dynamic reweighting, 2021.

Zhuang, J., Gong, B., Yuan, L., Cui, Y., Adam, H., Dvornik, N. C., sekhar tatikonda, s Duncan, J., and Liu, T. Surrogate gap minimization improves sharpness-aware training. In *International Conference on Learning Representations*, 2022. URL <https://openreview.net/forum?id=edONMAnhLu->.

Appendix

A. Visualization details

For each model, we re-compute the batch norm statistics by one forward-pass over the training set before evaluating it.

Linear interpolations To linearly interpolate between two sets of parameters θ and θ' , we parameterize the line connecting these two points by choosing a scalar parameter α , and defining the weighted average $\theta(\alpha) = (1 - \alpha)\theta + \alpha\theta'$.

2D Surface visualizations We choose the optimizer solution θ as center point of the plot, and two direction vectors, δ and η . Then, we plot the losses summed over the full training/test set as

$$f(\alpha, \beta) = \mathcal{L}(\theta + \alpha\delta + \beta\eta). \quad (7)$$

To yield δ, η , we first sample $\delta, \eta \sim \mathcal{N}(\mathbf{0}, \mathbf{I})$, orthogonalize η w.r.t. to δ using the Gram-Schmidt process (Deisenroth et al., 2020), and then filter-wise normalize them (Li et al., 2018). For both training settings (WRN on CIFAR100, and GIN on Code2), we use $\alpha, \beta \in [-1, 1]$. For WRN on CIFAR100, we discretize the 2D-grid 20 with equally-spaced steps in each dimension; for GIN on Code2 with 15 steps. For better readability, we cropped the WRN on CIFAR100 plots shown in Figure 3 after computing the losses.

B. Experimental details

B.1. Computer Vision

We mostly adapt the hyper-parameter values from Foret et al. (2021) for WRN-28-10 and PyramidNet-272, from Dosovitskiy et al. (2021) for ViT, and from (Tolstikhin et al., 2021) for MLP-Mixer models. We average all results across three random seeds.

B.1.1. SUPERVISED CLASSIFICATION

We train WideResNets (Zagoruyko & Komodakis, 2016) with 28 layers and width 10 (WRN28-10) and PyramidNet (Han et al., 2017) with 110 layers and widening factor $\alpha = 272$ (PyramidNet-272) from scratch. The Vision Transformer (ViT) base model with input patch size 16 (ViT-B/16) and MLP-Mixer base model with input patch size 16 (MLP-Mixer-B/16) start from pre-trained checkpoints available at https://console.cloud.google.com/storage/vit_models/. The reason for using pre-trained checkpoints for the ViT and MLP-Mixer models is that, due to their lack of some inductive biases inherent to CNNs, such as translation equivariance and locality, they do not generalize well when trained on insufficient amounts of data (Dosovitskiy et al., 2021). Table 4 shows the hyper-parameters for each architecture.

B.1.2. SELF-SUPERVISED LEARNING

Table 5 shows the hyper-parameters for each SSL method. We use implementations from the lightly package, available at <https://github.com/lightly-ai/lightly> (Susmelj et al., 2020).

B.2. Natural Language Processing

For the task of Open Domain Question Answering, we adapt the hyper-parameter values and the 100 retrieved passages for each question from Izacard & Grave, 2021. We report the Exact Match score of FiD-base model on Natural Questions (NQ) and TriviaQA test sets. For GLUE benchmark, we report Matthew’s Corr for CoLA, Pearson correlation coefficient for STSB, and accuracy for the the rest of the datasets. Results are all evaluated on the dev set of GLUE benchmark. We use the RoBERTa-base as our backbone language model, implemented with Huggingface Transformers (Wolf et al., 2020). Most of the task-specific hyper-parameter values are adapted from Aghajanyan et al., 2020.

Table 4. Hyper-parameters for Supervised Classification (SC): CIFAR- $\{10, 100\}$ (Table 1)

Hyper-Parameter	WRN28-10	PyramidNet-272	ViT-B/16	MLP-Mixer-B/16
Base Optimizer	SGD	SGD	SGD	SGD
Batch size	256	256	100	170
Data augmentation	Inception-style + Cutout (Devries & Taylor, 2017)			
Dropout rate			0.0	
Epochs	200	200	–	–
Gradient clipping norm	–	–	1.0	1.0
Learning rate schedule			cosine	
Peak learning rate	0.1	0.05	0.03	0.03
Steps	–	–	12500	12500
SGD Momentum			0.9	
Warmup steps	–	–	500	500
Weight decay	$5e-4$	$5e-4$	0.0	0.0
CIFAR-10				
SAM ρ	0.05	0.05	0.1	0.02
Averaging start E (SWA)	60%	60%	75%	90%
Averaging start E (WASAM)	90%	75%	75%	90%
CIFAR-100				
SAM ρ	0.1	0.1	0.2	0.05
Averaging start E (SWA)	60%	60%	75%	90%
Averaging start E (WASAM)	90%	75%	75%	90%

Table 5. Hyper-parameters for Self-Supervised Learning (SSL): CIFAR-10, ImageNette, results in (Table 1)

Hyper-Parameter	MoCo	SimCLR	SimSiam	BarlowTwins	BYOL	SwaV
Backbone Network	ResNet-18					
Base Optimizer	SGD					Adam
Data augmentation	SimCLR (Chen et al., 2020)					Multi-Crop (Caron et al., 2020)
Dropout rate				0.0		
Epochs				800		
Embedding dimensions				512		
KNN memory bank size				4096		
Learning rate schedule				cosine		
Peak learning rate			$6e-2$			$1e-3$
SGD Momentum			0.9			–
Weight decay			$5e-4$			$1e-6$
CIFAR-10						
Batch size				512		
Crop size			–			32
Gaussian blur				0%		
SAM ρ	0.01	0.01	0.01	0.05	0.01	0.05
Averaging start E (SWA)	75%	90%	75%	90%	60%	60%
Averaging start E (WASAM)	90%	90%	90%	90%	75%	90%
ImageNette						
Batch size				256		
Crop size			–			128, 64
Gaussian blur				50%		
SAM ρ	0.01	0.01	0.02	0.05	0.05	0.01
Averaging start E (SWA)	50%	90%	75%	75%	90%	50%
Averaging start E (WASAM)	50%	50%	90%	75%	90%	50%

B.3. Graph Representation Learning

We mostly adapt the hyper-parameter values from Hu et al. (2020) for GCN (Kipf & Welling, 2017), SAGE (Hamilton et al., 2017), and GIN (Xu et al., 2019), from Chen et al. (2021b) for (Lacroux et al., 2018) and ComplEx (Trouillon et al., 2016), and from Li et al. (2020) for DGCN. Due to high standard errors, we averaged the results of a few tasks more than three times, as mentioned in the following tables.

Table 6. Hyper-parameters for NPP tasks, results in Table 3.

Hyper-Parameter	SAGE	DGCN
NPP: OGB-Proteins		
Aggregation method	Mean	Softmax
Base optimizer	Adam	Adam
Convolution layer	SAGE	DyResGEN
Dropout rate	0.0	0.1
Hidden dimensions	256	64
Learning rate	0.01	0.001
Normalization layer	–	Layer norm
Number of epochs	2000	1000
Number of layers	3	112
Number of random seeds	5	3
Training cluster number	1	15
Weight decay	0.0	0.0
SAM ρ	0.01	0.02
Averaging start E (SWA)	90%	90%
Averaging start E (WASAM)	90%	90%
NPP: OGB-Products		
Aggregation method	Mean	Softmax
Base optimizer	Adam	Adam
Batch size	20000	–
Convolution layer	SAGE	Gen
Dropout rate	0.5	0.5
Evaluation cluster number	–	8
Learning rate	0.01	0.001
Hidden dimensions	256	128
Normalization layer	–	Batch norm
Number of epochs	30	50
Number of layers	3	14
Number of random seeds	5	3
Training cluster number	–	10
Weight decay	0.0	0.0
SAM ρ	0.01	0.02
Averaging start E (SWA)	90%	60%
Averaging start E (WASAM)	75%	90%

Table 7. Hyper-parameters for GPP: OGB-Code2, results in Table 3.

Hyper-Parameter	GCN	GIN
GPP: OGB-Code2		
Aggregation method	Mean	Mean
Base optimizer	Adam	Adam
Batch size	128	128
Convolution layer	GCN	GIN
Dropout rate	0.0	0.0
Learning rate	0.001	0.001
Hidden dimensions	300	300
Normalization layer	Batch norm	Batch norm
Number of random seeds	3	3
Number of epochs	15	30
Number of layers	5	5
Virtual node embeddings	True	True
Vocabulary size	5000	5000
Weight decay	0.0	0.0
SAM ρ	0.2	0.15
Averaging start E (SWA)	50%	50%
Averaging start E (WASAM)	50%	50%

Table 8. Hyper-parameters for GPP: OGB-Molpcba, results in Table 3.

Hyper-Parameter	GIN	DGCN
GPP: OGB-Molpcba		
Aggregation method	Mean	Mean
Batch size	512	512
Base optimizer	Adam	Adam
Convolution layer	GIN	GEN
Dropout rate	0.0	0.2
Learning rate	0.001	0.001
Normalization layer	Batch norm	Batch norm
Number of epochs	100	50
Number of layers	5	14
Number of random seeds	3	3
Hidden dimensions	300	256
Virtual node embeddings	False	True
Weight decay	0.0	0.0
SAM ρ	0.01	0.15
Averaging start E (SWA)	90%	75%
Averaging start E (WASAM)	90%	50%

Table 9. Hyper-parameters for LPP: OGB-Biokg, results in Table 3.

Hyper-Parameter	CP	Complex
GPP: OGB-Biokg		
Base optimizer	Adam	Adam
Batch size	500	500
Learning rate	0.1	0.1
Number of random seeds	3	3
Number of epochs	30	50
Rank	1000	1000
Regularizer	N3	N3
Weight decay	0.0	0.0
SAM ρ	0.1	0.05
Averaging start E (SWA)	50%	50%
Averaging start E (WASAM)	90%	50%

Table 10. Hyper-parameters for LPP: OGB-Citation2, results in Table 3.

Hyper-Parameter	GCN	SAGE
GPP: OGB-Citation2		
Aggregation method	Mean	Mean
Base optimizer	Adam	Adam
Batch size	256	512
Convolution layer	GCN	SAGE
Dropout rate	0.0	0.2
Hidden dimensions	256	256
Number of epochs	300	300
Number of layers	3	3
Number of random seeds	3	3
Normalization layer	–	–
Learning rate	0.001	0.0005
Virtual node embeddings	False	False
Weight decay	0.0	0.0
SAM ρ	0.02	0.01
Averaging start E (SWA)	75%	90%
Averaging start E (WASAM)	60%	90%